nature microbiology

ARTICLES

https://doi.org/10.1038/s41564-018-0303-7

Structure–function analysis of neutralizing antibodies to H7N9 influenza from naturally infected humans

Kuan-Ying A. Huang[1,2,17]*, Pramila Rijal[3,17], Haihai Jiang[4,5,17], Beibei Wang[6,7,8,17], Lisa Schimanski[3], Tao Dong[3,6], Yo-Min Liu[9], Pengxiang Chang[10], Munir Iqbal[10], Mu-Chun Wang[11], Zhihai Chen[8,12], Rui Song[8,12], Chung-Chi Huang[13], Jeng-How Yang[14], Jianxun Qi[4], Tzou-Yien Lin[1,2], Ang Li[7,8], Timothy J. Powell[3], Jia-Tsrong Jan[9], Che Ma[9], George F. Gao[4,15,16]*, Yi Shi[4,15,16]* and Alain R. Townsend[3,6]*

Little is known about the specificities and neutralization breadth of the H7-reactive antibody repertoire induced by natural H7N9 infection in humans. We have isolated and characterized 73 H7-reactive monoclonal antibodies from peripheral B cells from four donors infected in 2013 and 2014. Of these, 45 antibodies were H7-specific, and 17 of these neutralized the virus, albeit with few somatic mutations in their variable domain sequences. An additional set of 28 antibodies, isolated from younger donors born after 1968, cross-reacted between H7 and H3 haemagglutinins in binding assays, and had accumulated significantly more somatic mutations, but were predominantly non-neutralizing in vitro. Crystal structures of three neutralizing and protective antibodies in complex with the H7 haemagglutinin revealed that they recognize overlapping residues surrounding the receptor-binding site of haemagglutinin. One of the antibodies, L4A-14, bound into the sialic acid binding site and made contacts with haemagglutinin residues that were conserved in the great majority of 2016–2017 H7N9 isolates. However, only 3 of the 17 neutralizing antibodies retained activity for the Yangtze River Delta lineage viruses isolated in 2016–2017 that have undergone antigenic change, which emphasizes the need for updated H7N9 vaccines.

Avian influenza H7N9 virus emerged in humans in 2013 and has continued to cause outbreaks in China[1]. The 2016–2017 epidemic was the largest outbreak, and accounts for nearly 50% of the cases reported so far[1]. It was accompanied by significant geographical spread and the detection of highly pathogenic (HP) viruses containing a polybasic cleavage site, which could render them capable of spread beyond the lung[1–6]. Mutations associated with resistance to neuraminidase inhibitors have also been identified[7–11]. In addition, the A/Guangdong/17SF003/2016 HP virus was shown to transmit between ferrets, the animal model thought to be most predictive of spread between humans[2,12]. As a result of these findings H7N9 influenza is now potentially considered the most serious pandemic threat[13,14].

Molecular epidemiology has revealed two new genetic lineages among human H7N9 isolates: the Yangtze River Delta and the Pearl River Delta clades[15]. Ferret antisera have shown that these viruses are antigenically distinct from those of the 2013 outbreak[5,16]. As a result, in March 2017 the World Health Organization recommended new candidate vaccine viruses from the Yangtze River Delta lineage, including A/Hong Kong/125/2017 (a low pathogenic (LP) avian virus) and A/Guangdong/17SF003/2016 (an HP avian virus).

An interesting feature of the epidemiology of H7N9 infections in humans is the reduced mortality in those born after 1968, which correlates with the date that H3N2 viruses first appeared in the human population[1,17]. H3N2 and H7N9 influenza are both group 2 viruses, and share some antibody binding epitopes in their haemagglutinins[18–25] and T cell epitopes in their core proteins[26,27]. Both these responses can contribute to protection by passive transfer[18,21,23,25] or vaccination[27,28]. However, it is not clear to what extent a recall response to these shared epitopes occurs during natural H7N9 infection in humans, or if it contributes to protection.

These issues emphasize the need for a deeper understanding of the human immune response to H7N9 viruses. We isolated 73 H7-reactive monoclonal antibodies from four individuals of

[1]Division of Pediatric Infectious Diseases, Department of Pediatrics, Chang Gung Memorial Hospital, Taoyuan, Taiwan. [2]School of Medicine, Chang Gung University, Taoyuan, Taiwan. [3]Human Immunology Unit, Weatherall Institute of Molecular Medicine, University of Oxford, John Radcliffe Hospital, Oxford, UK. [4]CAS Key Laboratory of Pathogenic Microbiology and Immunology, Institute of Microbiology, Chinese Academy of Sciences (CAS), Beijing, China. [5]College of Veterinary Medicine, China Agricultural University, Beijing, China. [6]Center for translational Immunology, Chinese Academy of Medical Science Oxford Institute, Nuffield Department of Medicine, Oxford University, Oxford, UK. [7]Institute of Infectious Diseases, Beijing Ditan Hospital, Capital Medical University, Beijing, China. [8]Beijing Key Laboratory of Emerging Infectious Diseases, Beijing, China. [9]Genomics Research Center, Academia Sinica, Taipei, Taiwan. [10]The Pirbright Institute, Pirbright, Woking, UK. [11]Department of Cardiovascular Surgery, Min-Sheng General Hospital, Taoyuan, Taiwan. [12]Clinical and Research Center of Infectious Diseases, The National Clinical Key Department of Infectious Disease, Beijing Ditan Hospital, Capital Medical University, Beijing, China. [13]Department of Pulmonary and Critical Care Medicine, Chang Gung Memorial Hospital, Taoyuan, Taiwan. [14]Division of Infectious Diseases, Department of Medicine, Chang Gung Memorial Hospital, Taoyuan, Taiwan. [15]Shenzhen Key Laboratory of Pathogen and Immunity, Shenzhen Third People's Hospital, Shenzhen, China. [16]Center for Influenza Research and Early-Warning, Chinese Academy of Sciences, Beijing, China. [17]These authors contributed equally: Kuan-Ying A. Huang, Pramila Rijal, Haihai Jiang, Beibei Wang. *e-mail: arthur1726@cgmh.org.tw; gaof@im.ac.cn; shiyi@im.ac.cn; alain.townsend@imm.ox.ac.uk

different ages with acute H7N9 infections in 2013–2014. Seventeen out of 73 antibodies neutralized influenza coated in H7 haemagglutinin related to the challenge virus (A/Anhui/1/2013). Only three neutralized pseudotypes coated in H7 from 2016–2017 isolates. We analysed the crystal structures of three antibodies that neutralized A/Anhui/1/2013 and showed that they bind within or close to the sialic acid binding site. One of these (L4A-14) has a binding footprint that is conserved in the great majority of recent H7N9 isolates, and was therapeutic for both 2013 and 2017 H7N9 viruses in a murine infection model. Antibodies that cross-reacted in binding to H3 HA, with variable region sequences that suggest a recall response, were abundant (28 of 60) in the three donors born after 1968, but were absent (0 of 13) from the donor born earlier.

Our results show that, in response to natural infection with H7N9 influenza, humans make rare highly protective neutralizing antibodies to the globular head of H7 haemagglutinin; in addition, donors born after 1968 make a recall response to epitopes in both the globular head and stem shared between H3 and H7 haemagglutinins. These results are similar to those obtained from individuals vaccinated with an H7 live attenuated vaccine and boosted with a subunit vaccine[29,30], and in response to DNA priming and subunit boost[25]. The low frequency (3 of 17) of neutralizing antibodies generated by natural infection in humans in 2013–2014 that cross-neutralize viruses isolated in 2016–2017 is consistent with convalescent serology and ferret serology[5,16], and demonstrates the extent of antigenic change in recent H7N9 isolates.

Results

H7-reactive antibodies induced by natural infection. Four donors, referred to as donors L, K, Z and W, were diagnosed with H7N9 influenza infection in 2013 and 2014 (Table 1).

Convalescent sera from the donors revealed several points of interest (Fig. 1). The sera of all four donors showed a strong neutralizing titre (>1:2,048) to single cycle influenza (S-FLU) pseudotypes[31] coated in haemagglutinin from recent seasonal viruses H3 A/Victoria/210/2009 and H1 A/England/195/2009. By contrast, only the two older donors (aged 86 and 39 years) showed reactivity with the H3 from X31 A/Aichi/2/1968. The two older donors who became ill with pneumonia from H7N9 A/Anhui/1/2013 infection developed high titre neutralizing antibody to this virus (>1:1,024), whereas the two younger donors who had mild respiratory illnesses developed low titre antibodies (~1:64). The sera were tested on pseudotypes coated in H7 haemagglutinin from five recent isolates from 2016–2017. The sera from the two older donors reacted with three of the pseudotypes with an 8–16-fold reduction in titre, whereas the two younger donors showed minimal or no reactivity. None of the sera retained any detectable neutralization of A/Taiwan/1/2017 or A/Guangdong/8H324/2017. These two viruses have acquired new N-linked glycosylation sites on the globular head of HA at positions N118 (128 in H3 numbering[32]) and N148 (158a in H3 numbering[32,33]), respectively. Both glycosylation sites are positioned in the antigenic site B, the latter in the equivalent position to the recent glycosylation site of the seasonal H3 haemagglutinin on the B loop at N158. The loss of reactivity of the sera with these haemagglutinins therefore suggests that the sera are composed predominantly of antibodies to the antigenic site B. The control anti-stem antibody MEDI8852[21] neutralized all the pseudotypes to some level except A/Guangdong/8H324/2017. This was not due to lack of binding, and represents a rare example of loss of in vitro neutralization by this antibody (Supplementary Fig. 1).

To explore the specificities and neutralization breadth of the H7-reactive antibody repertoire, we identified circulating plasmablasts during the acute phase of infection by flow cytometry and sorted single cells to generate human IgG monoclonal antibodies. A total of 254 monoclonal antibodies were screened for binding H7 HA from A/Anhui/1/2013. Of these, 13 of 49 from donor L, 45 of 111 from donor K, 14 of 86 from donor Z and 1 of 8 antibodies from donor W bound specifically to Madin-Darby canine kidney epithelial-human 2,6-sialyltransferase (MDCK-SIAT1) cells[34] transduced

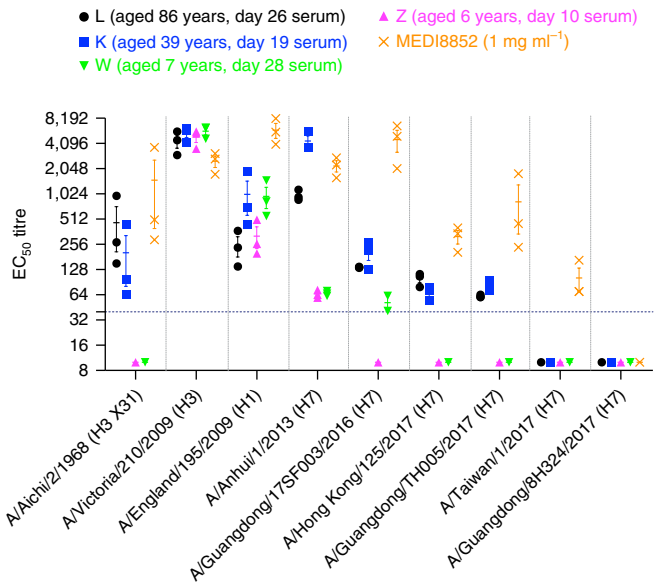

Fig. 1 | Neutralization titres of convalescent sera from donors with laboratory-confirmed H7N9 infection. Convalescent sera were collected from donors and tested against H1, H3 and H7 pseudotypes. The anti-haemagglutinin (HA) stem MEDI8852[21] reference antibody was included. Neutralization titres are expressed as reciprocal 50% effective concentrations (EC_{50}) derived by linear interpolation from neighbouring points in the titration curve, and the lines represent mean ± s.e.m. All experiments were independently repeated three times ($n = 3$). Each symbol represents an independent measurement and some measurements overlap. Titres less than the starting dilution of 1:40 are placed at the base of the figure.

Table 1 | Summary of 73 human MAbs to H7

Donor	Age (yr)	Gender	Clinical diagnosis	Sample day	Total MAbs isolated	H7-reactive	H7-neutralizing	H3-reactive	H3-neutralizing
L	86	Male	Pneumonia requiring extracorporeal membrane oxygenation	D21, D26	49	13	7	0	0
K	39	Male	Pneumonia	D11, D19	111	45	8	20	0
Z	6	Male	Mild respiratory tract infection	D7, D10	86	14	1	7	6
W	7	Female	Mild respiratory tract infection	D13, D28	8	1	1	1	1

Table 2 | Haemagglutination inhibition and neutralization by representative H7-reactive antibodies on pseudotypes and wild-type viruses

		Haemagglutination-inhibition				Neutralization												
						2013 avian H7			2016–2017 avian H7						2003 avian H7		Seasonal H3	
Antibody	Vh	H7 A/Anhui/1/2013	H7 A/Taiwan/1/2017	H3 X217 (A/Victoria/361/2011)	H3 X31 (A/Aichi/2/1968)	H7 A/Anhui/1/2013	H7 A/Shanghai/1/2013	H7 A/Anhui/1/2013 *wt virus*	H7 A/Guangdong/17SF003/2016	H7 A/Taiwan/1/2017	H7 A/Hong Kong/125/2017	H7 A/Guangdong/TH005/2017	H7 A/Guangdong/TH005/2017 *wt virus*	H7 A/Guangdong/8H324/2017	H7 A/Netherlands/219/2003	H7 A/New York/107/2003	H3 X217 (A/Victoria/361/2011)	H3 X31 (A/Aichi/2/1968)
H7-specific head																		
L4A-14	3-30	+++	+++	–	–	+++	+++	++	+++	+++	+++	+++	++++	–	–	–	–	–
L3A-44	4-34	+++	–	–	–	+++	++	+	–	–	+	±	+	–	–	–	–	–
L4B-18	3-23	+	–	–	–	++	+++	+	ND	ND	ND	–	–	ND	–	–	–	–
K9B-122	4-59	++	–	–	–	++	+++	ND	–	–	–	±	ND	–	–	++	–	–
L11B-46	1-3	++	–	–	–	++	–	ND	–	–	+	–	ND	–	–	–	–	–
L9B-26	1-18	++	–	–	–	+++	–	ND	+	±	+	+	ND	–	–	–	–	–
L12B-36	4-34	+++	–	–	–	++	–	ND	–	–	–	–	ND	–	–	–	–	–
H7/H3 cross-reactive stem																		
Z3B2	3-53	–	–	–	–	–	–	ND	ND	ND	ND	–	ND	ND	–	–	+	+
Z3A8	3-23	–	–	–	–	–	–	ND	ND	ND	ND	ND	ND	ND	–	–	+	+
H7/H3 cross-reactive head																		
W3A1	4-39	+	++	±	–	++	++	ND	+++	++	++	++	ND	–	–	++	+	–
Z1B10	3-20	+	++	+	–	+	++	ND	++	+	+	++	ND	+	–	+	+	–
Z3A9	3-30	–	–	+	–	–	–	ND	ND	ND	ND	–	ND	ND	–	–	+	–

Haemagglutination-inhibition activity is defined as the minimal concentration of the antibody required to prevent haemagglutination. The neutralizing activity is defined as the EC_{50} value. –, negative; ±, 30–50 μg ml^{-1}; +, 2–30 μg ml^{-1}; ++, 0.2–2 μg ml^{-1}; +++, 20–200 ng ml^{-1}; ++++, <20 ng ml^{-1}. Wild-type H7 viruses are indicated by *wt*, the other H7 viruses are single cycle influenza pseudotyped with the indicated H7 proteins. H3 X217 and H3 X31 are replication competent vaccine viruses. ND, not determined. Vh, variable gene segment of the heavy chain variable domain.

to express recombinant haemagglutinin from A/Anhui/1/2013 (Table 1 and Supplementary Table 1).

The 73 H7-reactive antibodies can be categorized into two major groups based on their binding and neutralizing activities: 45 of 73 bound specifically H7 haemagglutinin and 15 of these neutralized H7-coated virus; 28 of 73 bound to both H7 and H3 haemagglutinins, and of these only two neutralized H7- and H3-coated viruses, but five additional antibodies neutralized modern H3 viruses (Table 1 and Supplementary Table 1). Clonal expansions of H7-reactive B cells were observed within individual donor repertoires, but each H7-reactive antibody had a unique sequence of rearranged variable, diversity and joining (VDJ) gene segments in the heavy- and light-chain variable domain when combined with somatic mutations (Supplementary Table 2).

H7-specific antibodies induced by natural infection. As shown in Table 2, seven representative H7-specific antibodies (that failed to bind H3 haemagglutinin) neutralized pseudotypes coated in A/Anhui/1/2013 HA, and inhibited haemagglutination by these viruses (Supplementary Fig. 1). Three failed to neutralize or weakly neutralized viruses coated with other H7 haemagglutinins (including the closely related A/Shanghai/1/2013), and were not studied further. Four antibodies (L4A-14, L3A-44, L4B-18 and K9B-122) cross-reacted to some level on haemagglutinin from more distantly related H7 isolates (Table 2). Only L4A-14 neutralized four of the five pseudotypes coated in haemagglutinin from several recent H7N9 viruses tested, including A/Guangdong/17SF003/2016, A/Taiwan/1/2017, A/Hong Kong/125/2017 and A/Guangdong/TH005/2017 with EC_{50} values less than 200 ng ml^{-1} (Table 2). Neutralization of the pseudotypes was correlated with inhibition of haemagglutination. The sequences of their V_H genes were close to germline, with few or absent amino acid substitutions (L4A-14 (five substitutions), L3A-44 (five substitutions), L4B-18 (one substitution) and K9B-122 (six substitutions)) indicating that this subset had not been selected from a memory population and arose most probably through a first exposure to H7 haemagglutinin.

Both L4A-14 and L3A-44 neutralized the two wild-type viruses tested (A/Anhui/1/2013 and A/Guangdong/TH005/2017) in vitro, but L4A-14 required 3 logs less antibody to neutralize the 2017 virus (Supplementary Fig. 2). Antibody L4A-14 was the most potent and had the highest apparent binding affinity (KD 16.6nM, Supplementary Fig. 3).

L4A-14 was applied to the selection of neutralization-resistant viruses from a laboratory reassortant virus based on A/Puerto Rico/8/1934. Mutation N149D (158b in H3 numbering[32,33]) in the antigenic site B, close to the sialic acid binding site, abolished neutralization. This mutation was found in 11 of 1,383 sequences in the GISAID database (Supplementary Table 3). This correlates with loss of recognition of the A/Guangdong/8H324/2017 haemagglutinin (Table 2), which has a unique glycosylation site at N148 (158a in H3 numbering) as a result of the combined substitutions D148N with A150T. This mutation combination occurs in only 2 of 1,383 H7 sequences in the GISAID database (Supplementary Table 3).

To further investigate the functional activities of H7-neutralizing antibodies and map the relevant epitopes, three antibodies that neutralized A/Anhui/1/2013 and A/Shanghai/1/2013—L4A-14, L4B-18 and L3A-44—were selected for crystallization.

H7-specific neutralizing antibodies bind the receptor-binding site in the globular head domain of A/Anhui/1/2013 haemagglutinin. The L4A-14/H7 complex structure reveals that the antibody recognizes the region surrounding the receptor-binding site (RBS) in the head domain of the H7 protein (Fig. 2a). L4A-14 uses both its heavy and light chains to engage the H7 protein, with a long HCDR3 loop inserting into the RBS. The heavy chain (including HCDR1, HCDR2 and HCDR3) contributes to the interactions of 138 atom-to-atom contacts, while the light chain (including LCDR1, LCDR2 and LCDR3) contributes less to the interaction with 96 atom-to-atom van der Waals contacts. The epitopes cover three secondary elements, the 120-loop (the 130-loop in H3 numbering), the

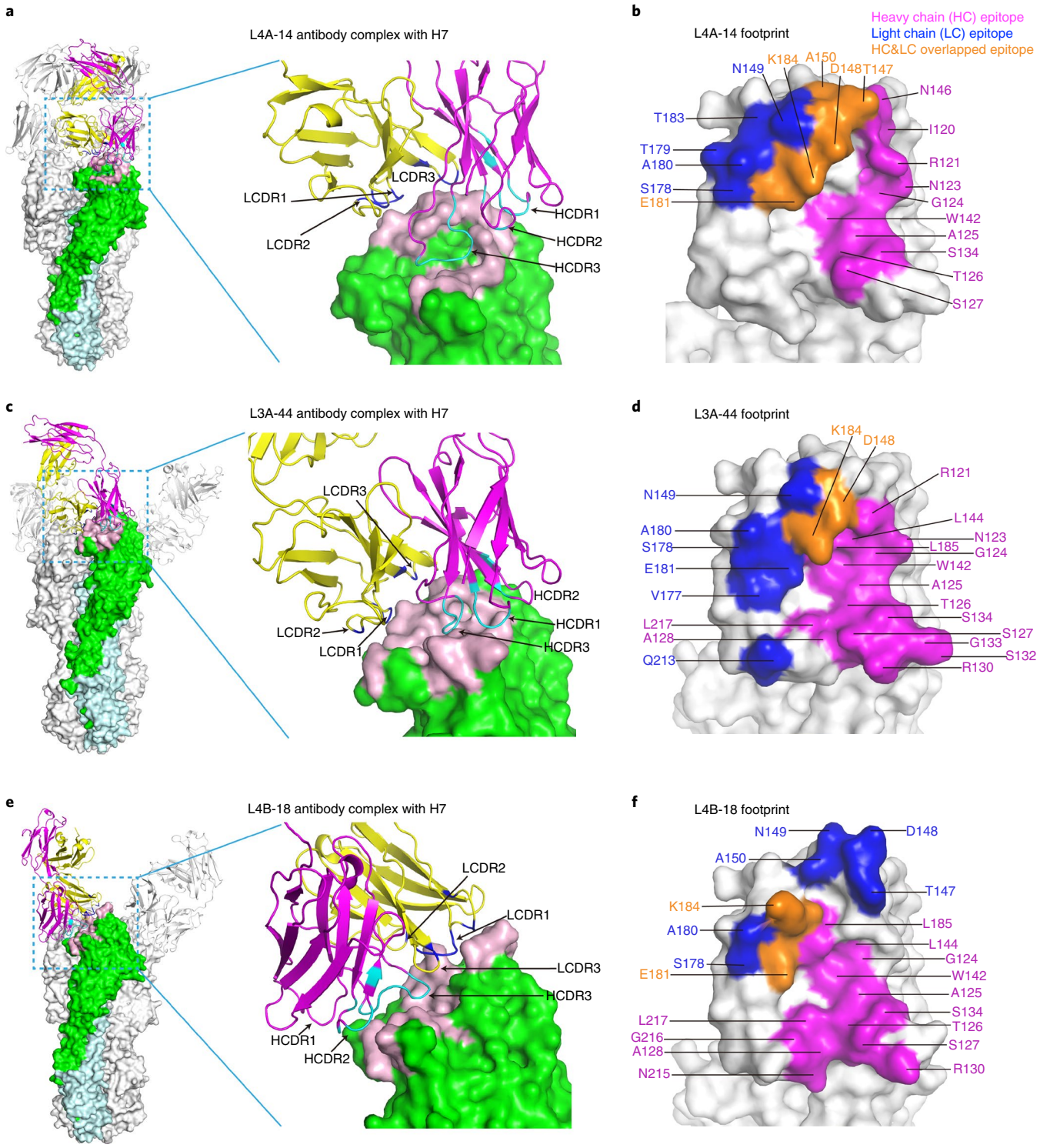

Fig. 2 | Structures of L4A-14/H7, L3A-44/H7 and L4B-18/H7 complexes. a,**c**,**e**, Overall structures of L4A-14/H7 (**a**), L3A-44/H7 (**c**) and L4B-18/H7 (**e**) complexes, displayed in a cartoon representation. The L4A-14, L3A-44 and L4B-18 Fab (heavy chain in magenta, light chain in yellow) bind the globular head domain of A/Anhui/1/2013 haemagglutinin. The HA1 head subunit is coloured green, the HA2 subunit light blue, and the epitope pink. **b**,**d**,**f**, The footprints on H7 of Fab L4A-14 (**b**), L3A-44 (**d**) and L4B-18 (**f**) are mapped on the haemagglutinin surface. The epitope residues that are contacted by the heavy or light chain are coloured in purple or blue, respectively (numbering from the first residue in the mature H7 protein[32]). The overlapping residues that are contacted by both heavy and light chains are in orange. HCDR1–3, heavy chain complementarity-determining regions 1–3; LCDR1–3, light chain complementarity-determining regions 1–3; HC, heavy chain; LC, light chain.

140-loop (the 150-loop in H3 numbering) and the 180-helix (the 190-helix in H3 numbering). Details of the contact amino acids in the epitope are shown in Fig. 2b.

For the L3A-44/H7 complex structure, the antibody similarly recognizes the region surrounding the RBS. L3A-44 uses both its heavy chain (including HCDR1, HCDR2 and HCDR3) and light

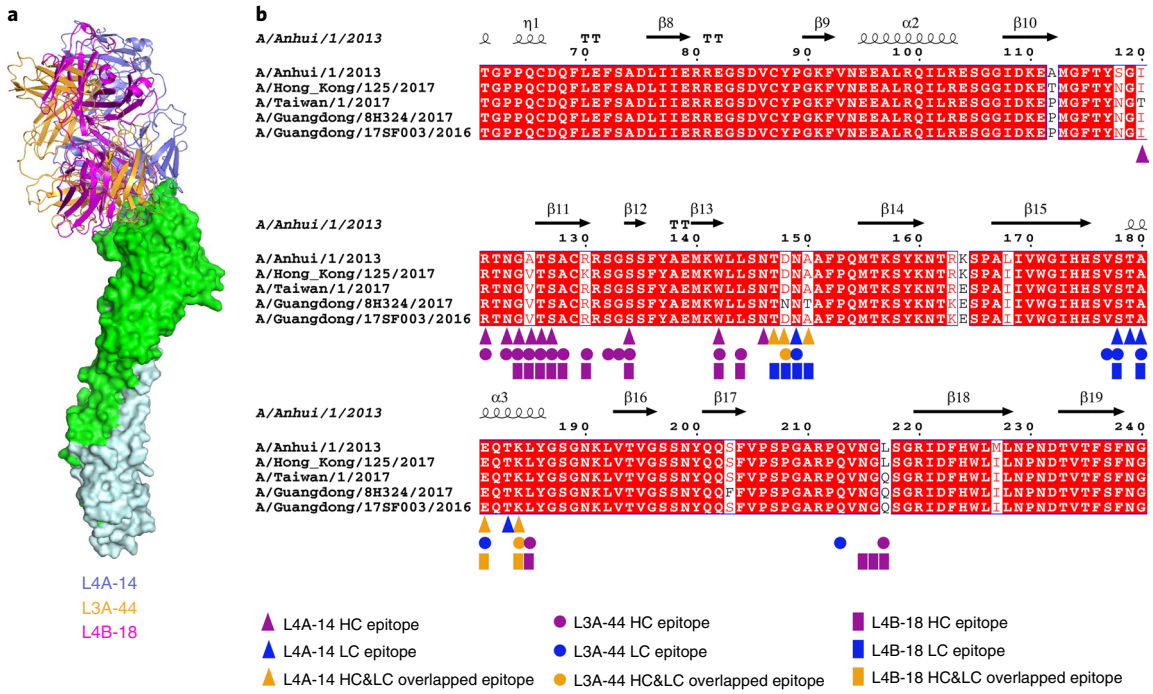

Fig. 3 | Comparison of epitope residues recognized by L4A-14, L3A-44 and L4B-18 antibodies. a, Antibody L4A-14 (in blue) has a more straight-on binding orientation than the L4B-18 (magenta) and L3A-44 (orange) antibodies. **b**, Haemagglutinin residues contacted by L4A-14 (triangles), L3A-44 (circles) and L4B-18 (squares) are mapped onto a structure-based sequence alignment of H7 haemagglutinins (A/Anhui/1/2013, A/Hong Kong/125/2017, A/Taiwan/1/2017, A/Guangdong/8H324/2017 and A/Guangdong/17SF003/2016). Unique residues are highlighted with white boxes. Numbering is taken from the first amino acid of the mature H7 protein[32].

chain (including LCDR1, LCDR2 and LCDR3) to bind the H7 protein (Fig. 2c). The heavy chain contributes to the interaction with 164 contacts, while the light chain only contributes 54 contacts. The epitopes cover four secondary elements, including the 120-loop, 140-loop, 180-helix and 210-loop. Detailed epitope residues are referred to Fig. 2d.

For the L4B-18/H7 complex structure, the antibody also mainly recognizes the epitopes surrounding the RBS. L4B-18 uses both its heavy chain (including HCDR2 and HCDR3) and light chain (including LCDR2, FR3 and LCDR3) to contact the H7 protein (Fig. 2e). The heavy chain contributes to the interaction with 109 contacts, while the light chain contributes to the interaction with 87 contacts. The region of contact covers four secondary elements of the H7 protein, including the 120-loop, 140-loop, 180-helix and 210-loop. Detailed epitope residues are referred to Fig. 2f.

Comparison of these three antibodies shows that the L4A-14 has a more straight-on binding orientation than the L4B-18 and L3A-44 antibodies (Fig. 3a). Sequence alignment also shows that the epitope residues of these three antibodies are largely overlapped (Fig. 3b). L4A-14 uniquely recognizes the residue at position 120, whereas L4B-18 and L3A-44 uniquely contact the residues at positions R130 and L217 (226 in H3 numbering[32,33]), which has been replaced with Q217 in recent isolates (Fig. 3b and Supplementary Table 3).

The footprint of the most potent antibody L4A-14 is conserved in the great majority of recent H7N9 viruses that have caused human infections (Fig. 3b, Supplementary Table 3 and Supplementary Table 4). The antibody selection experiment with neutralization-resistant strains showed that the N149D mutation could abolish the neutralizing activity of L4A-14, which could be explained by electrostatic repulsion from the negative-charged residue D95 in the LCDR3 loop (Supplementary Fig. 4). In addition, the introduction of a glycosylation site at N148 via two mutations D148N and A150T can also generate a steric clash with the CDR loops of the antibody (Fig. 2a,b).

H7-neutralizing antibodies are protective in vivo for prophylaxis and therapy. We tested the efficacy in prophylaxis and therapy of neutralizing antibodies against 2016–2017 epidemic virus in mice. Figure 4a shows that L4A-14 conferred 100% protection at a dose of 20 mg kg^{-1}. By contrast, a higher dose of 30 mg kg^{-1} was required for L3A-44 to be 100% protective, and L4B-18 failed to protect mice from lethal infection. Although mice were protected from lethal infection by both L4A-14 and L3A-44, the L4A-14 treated animals showed less weight loss and quicker recovery. In Fig. 4b these antibodies have also been tested in a therapeutic model, and we observed that both L4A-14 (at 10 mg kg^{-1}) and L3A-44 (at 20 or 30 mg kg^{-1}) were able to fully protect mice from lethal infection with A/Guangdong/TH005/2017.

We also tested the prophylactic efficacy of neutralizing antibodies (at 20 mg kg^{-1}) against 2013 epidemic virus in mice. Figure 4c shows that L4A-14 and K9B-122 conferred 100% protection from lethal infection, with L3A-44 being partially (83%) protective for the infected mice. Mice receiving L4A-14 showed minimal weight loss after infection, and body weight was gradually restored by 5 days post infection. By contrast, mice treated with L3A-44 and K9B-122 lost more weight but recovered. Untreated control mice continued to lose weight and succumbed to infection by day 8. These results demonstrated that all three antibodies substantially decreased the mortality of mice infected with 2013 H7N9 virus, with L4A-14 being the most effective.

Antibodies L4A-14 and K9B-122 were further tested in a therapeutic model, with 20 mg kg^{-1} of each antibody being administered 24 h after infection, and we observed 100% survival only with antibody L4A-14 (Fig. 4d).

Antibodies that cross-react between H7 and H3 haemagglutinins. Of the 73 antibodies we isolated, 28 of 60 from the three donors born after 1968 cross-reacted in binding assays with H3

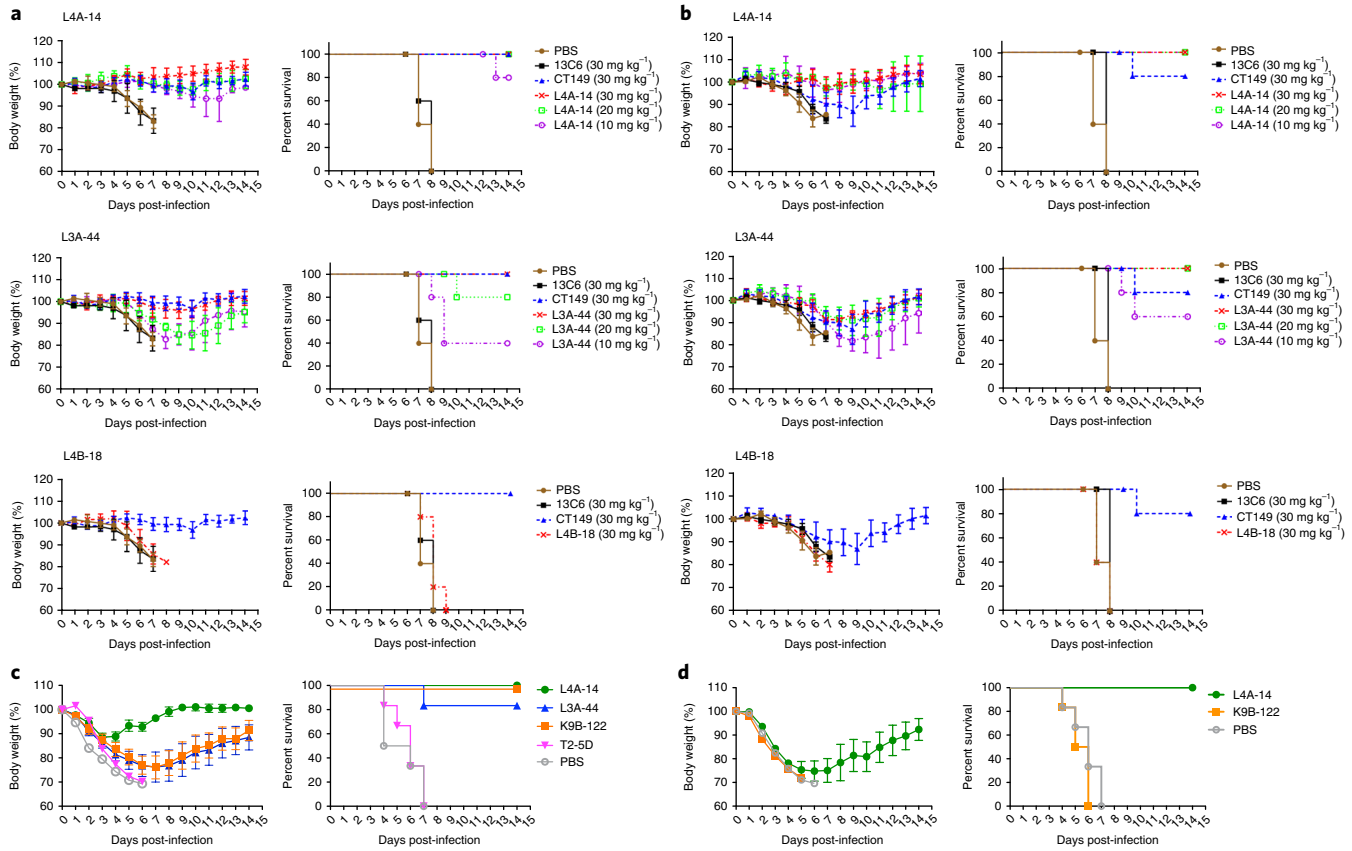

Fig. 4 | Protection against lethal infection with H7N9 in mice by antibodies. a,**b**, In vivo prophylactic (**a**) and therapeutic (**b**) effects of neutralizing antibodies L4A-14, L3A-44 and L4B-18 against high pathogenic H7N9 A/Guangdong/TH005/2017 (an HP avian virus related to A/Guangdong/17SF003/2016) infection in BALB/c mice ($n=5$ per group). **c**,**d**, In vivo prophylactic (**c**) and therapeutic (**d**) effects of neutralizing antibodies L4A-14, L3A-44 and K9B-122 against H7N9 A/Taiwan/1/2013 (a 2013 H7N9 virus related to A/Anhui/1/2013) infection in BALB/c mice ($n=6$ per group). A single dose of antibody or control was administered 24 h before or after intranasal infection in the prophylactic or therapeutic experiment, respectively. The experiments were performed with PBS, anti-Ebola IgG antibody 13C6, anti-H1 IgG antibody T2-5D or cross-reactive anti-HA stem antibody CT149 as controls. Body weight data are shown as group mean ± s.e.m. of the percent in weight of surviving animals relative to their starting weights. d.p.i., day post-infection.

haemagglutinin (A/Victoria/361/2011). By contrast, 0 of 13 antibodies from donor L, born before 1968, cross-reacted ($P=0.0013$, two-tailed Fisher's exact test) (Table 1 and Supplementary Table 1).

Only 2 of the 28 cross-reactive antibodies, W3A1 and Z1B10, neutralized H7-coated pseudotypes in our assays (Supplementary Table 1 and Table 2). Antibodies W3A1 and Z1B10 bound H3 weakly (Supplementary Fig. 1), but neutralized modern H3N2 vaccine virus X217 (containing H3 and N2 from A/Victoria/361/2011). Both antibodies inhibited haemagglutination by H7 viruses (Table 2), indicating that they bind epitopes in the haemagglutinin head close to the sialic acid binding site. They were unusual in being germline in their V_H sequences without any evidence of affinity maturation and no amino acid substitutions in their V_H sequence (Supplementary Table 2). An additional H7-binding antibody Z3A9 also bound H3 weakly, inhibited haemagglutination and neutralized a modern H3 virus in vitro, but not any H7 viruses (Table 2 and Supplementary Fig. 1). We classify it also as a head-binding antibody.

The remaining 25 H7/H3 cross-reactive antibodies bound H3 as strongly as H7 (represented by Z3B2 and Z3A8 in Supplementary Table 1 and Supplementary Fig. 1). Five H7/H3 cross-reactive antibodies neutralized an H3N2 virus, while most were not neutralizing in vitro (Supplementary Table 1). One of them (Z3B2) was shown to compete with anti-stem antibody MEDI8852 for binding (Supplementary Fig. 5), indicating that it recognized an overlapping epitope in the haemagglutinin stem. Cross-reactive antibodies Z3A8 and Z3B2 neutralized H3N2 virus from 2011 (X217 A/Victoria/361/2011) and 1968 (X31 A/Aichi/2/1968) (Table 2). Both antibodies were also protective in prophylaxis against X31 infection in BALB/c mice (Supplementary Fig. 6a). In addition, Z3B2 was protective in prophylaxis against H1N1 A/California/07/2009 (X179A) infection in DBA/2 mice (Supplementary Fig. 6b). These results suggest that Z3B2 is a group 1 and 2 cross-reactive anti-stem antibody.

Comparison of the sequences of H7-specific and H7/H3 cross-reactive antibodies. The 45 H7-specific antibodies harboured an average of 7 ± 5 and 4 ± 3 non-silent nucleotide mutations in the heavy and light variable domain, respectively, whereas the 28 H7/H3 cross-reactive antibodies harboured 16 ± 8 and 10 ± 6 mutations, respectively (H7-specific versus cross-reactive, $P<0.0001$ for both heavy and light chains, two-tailed Mann–Whitney test) (Supplementary Fig. 7). This highly significant difference suggests that, following a first exposure to H7 haemagglutinin, two populations of B cells are selected: a group directed at the H7 globular head that are predominantly H7-specific represented by L4A-14, with occasional clones with wider cross-reactivity for H3 such as W3A1 and Z1B10, derived from primary activated B cells, and a second H7/H3 cross-reactive group selected from memory B cells previously primed by seasonal H3 influenza.

Of the 28 H7/H3 cross-reactive antibodies we isolated we found one encoded by Vh1-18, none by Vh6-1, seven by Vh1-2 and six by Vh3-53, and others encoded by six additional Vh genes (Supplementary Table 2), suggesting there may be some preferential use of Vh1-2 and Vh3-53 in the H7/H3 cross-reactive antibodies elicited by infection[25]. However, our Vh1-2 and all but one (Z3B2) of the Vh3-53 encoded antibodies express a shorter heavy chain CDR3 than the canonical 18 residues described for the vaccine response[25]. Z3B2 is typical of the group 1 and 2 cross-reactive stem-binding antibodies encoded by Vh3-53/Dh3-9/Jh6, Vl2-8 with an HCDR3 length of 18 amino acids (ARFLVLRYFDWPNYAMDV).

Discussion

Convalescent sera from our four donors who were naturally infected with 2013–2014 H7N9 viruses showed a greatly reduced neutralizing response to the fifth-epidemic Yangtze River Delta lineage viruses (Fig. 1). This observation emphasizes the degree of antigenic change that has occurred in the H7N9 viruses between 2013 and 2017, and warrants investigation of the human antibody repertoire.

We have characterized a panel of H7-reactive human monoclonal antibodies from donors naturally infected with 2013–2014 H7N9 virus and have shown that powerful and broadly protective antibodies to the globular head domain, despite minimal affinity maturation (five amino acid substitutions in V_H and two in V_L for L4A-14; Supplementary Table 2), can be induced by natural infection in a naive donor. Low levels of somatic mutation are characteristic for similar antibodies isolated after H7 subunit vaccination[30,33], and imply that these antibodies are part of a primary response.

Although the inhibitory substitutions at residues 148–150 (158–160 in H3 numbering[32]) would classify L4A-14 as a site B binding antibody, the crystal structure reveals that it straddles the sialic acid binding site, and thus does not fit the classical classification[35]. The interaction of L4A-14 with the sialic acid binding site is similar to the post infection antibody HNIgGA6[36]. An important difference is that HNIgGA6 is sensitive to changes at V177G and L217Q (186 and 226 in H3 numbering), which are not part of the L4A-14 binding footprint. The L217Q variation would not change the dual receptor binding property for sialic acids[37] and tends to be Q in the 2016–2017 HP viruses[2,12]. L4A-14 antibody neutralized four of five recent H7N9 viruses and was effective as therapy in mice for the HP A/Guangdong/TH005/2017 (with Q217) (Table 2 and Fig. 4). These results suggest that L4A-14 is a good candidate as a therapeutic antibody for human infections with the H7N9 viruses now circulating, perhaps combined with a protective antibody to the stem or N9 neuraminidase to minimize the selection of resistant variants.

The two other antibodies we selected for crystallization—L4B-18 and L3A-44—had overlapping binding footprints despite each being encoded by different V_H genes (Fig. 3b and Supplementary Table 2). Neither was able to neutralize as many recent Yangtze River Delta viruses as L4A-14 (Table 2). Our structural analysis has shown that both L4B-18 and L3A-44 contact the 210-loop (the 220-loop in H3 numbering), especially residue 217 (226 in H3 numbering). This binding feature determines that both antibodies are susceptible to mutation at position 217, and may explain why both antibodies fail to neutralize recent Yangtze River Delta viruses because substitution L217Q occurred in most of them (Fig. 3b). The three antibodies for which we obtained structures were isolated from the same donor. It will be of interest to compare the structures of the neutralizing antibodies from younger donors, such as W3A1 and Z1B10, in the future.

We found a large fraction of antibodies (28 of 60) that cross-reacted in binding with H3 haemagglutinin in donors born after 1968 (Table 1 and Supplementary Table 1). It is interesting to note that the serology shown in Fig. 1 shows that donor L (who was born well before 1968) must have been exposed to H3 viruses as an adult, and made antibodies to them, but did not produce any plasmablast-derived monoclonal antibodies (0 of 13) that cross-reacted between H7 and H3 haemagglutinins. Although with only four donors we are cautious not to over-interpret this result, we speculate that such cross-reactive antibodies may be primed predominantly in individuals whose first exposure to influenza was with an H3 virus.

These proportions are similar to the results of ref. [30] from an analysis of 20 human monoclonal antibodies from donors aged 18–49 years in a clinical trial of H7 (A/Anhui/1/2013) live attenuated vaccine followed by a subunit H7 boost[29]. The great majority of these participants would have been born after 1968, and 10 of 20 antibodies cross-reacted on H3 haemagglutinin. They went on to show that these antibodies could show low-level protection (associated with greater weight loss) in mice. Similarly, non-neutralizing serum pools from donors immunized with the H7 subunit vaccine Panblok[23] provided a low level of protection from H7 challenge (associated with >20% weight loss and 60% survival) in comparison to a pool of neutralizing sera (5% weight loss and 100% survival). These and other results defining H7/H3 cross-reactive monoclonal antibodies to the haemagglutinin stem from H7 naive donors[19,20,25] suggests that such antibodies can provide a level of protection against H7N9 infection and are consistent with the observation that mortality is significantly lower in individuals born after 1968[17]. However, this association needs more investigation to provide a definitive causal relationship.

We also noted a small subgroup of H7/H3 cross-reactive antibodies, including W3A1 and Z1B10, that bound the globular head of H7 and H3 haemagglutinins (Table 2 and Supplementary Fig. 8). They differed from the majority of H7/H3 cross-reactive antibodies in that their V gene sequences were essentially germline. Only a few broadly neutralizing antibodies binding epitopes in the haemagglutinin head have been reported[38–41]. In each case an extended HCDR3 loop allows these antibodies to insert into the conserved sialic acid binding site. Sequence analysis shows that W3A1 contains a long HCDR3, but Z1B10 has a short one. Further structural analysis will help to elucidate the antigenic breadth and potency of these broadly reactive antibodies.

In summary, we have shown that humans naturally infected with H7N9 influenza make an antibody response that includes rare broadly neutralizing and highly protective antibodies that bind the receptor-binding region of the H7 haemagglutinin, and common non-neutralizing antibodies, many of which cross-react with H3 haemagglutinin, and which may also be protective, at least in prophylaxis. These results are closely related to studies of donors after H7N9 live attenuated or subunit vaccination[25,30,33], which suggests that natural H7N9 infection and vaccination are expanding similar repertoires of B cells. This may bode well for the development of effective antibody-inducing vaccines.

Methods

Ethics. The study was in compliance with good clinical practice guidelines and the Declaration of Helsinki. The protocol was approved by the Research and Ethics Committee of Chang Gung Memorial Hospital, Beijing Ditan Hospital and Weatherall Institute of Molecular Medicine. All subjects provided written informed consent.

Patients and samples. Four patients, two adults and two children who were diagnosed with acute H7N9 infections were prospectively enrolled in Ditan Hospital, Beijing, China and Chang Gung Memorial Hospital, Taoyuan, Taiwan, in 2013 and 2014. Acute H7N9 infection was diagnosed by a positive laboratory test for H7N9 by RT–PCR and/or viral isolation in the respiratory specimens with or without the presence of fever and respiratory illnesses. The demographic and clinical features of patients are shown in Table 1. Whole bloods were taken during the acute and convalescent stage of infection.

Monoclonal antibodies. Peripheral blood mononuclear cells were freshly isolated and resuspended in staining buffer (PBS/1% fetal calf serum). One aliquot of cells (~1×10^6 cells in 100 µl of staining buffer) was incubated with antibodies, including Pacific Blue anti-CD3 (clone UCHT1, BD), fluorescein isothiocyanate (FITC) anti-CD19 (clone HIB19, BD), phycoerythrin-cyanin-7 anti-CD27

(clone M-T271, BD), allophycocyanin-cyanine tandem anti-CD20 (clone L27, BD), PE-Cy5 anti-CD38 (clone HIT2, BD) and allophycocyanin anti-IgM (clone G20-127, BD), for 30 min at 4 °C. After incubation, cells were washed twice with staining buffer and passed through a cell strainer to avoid clogs in the cytometer. The gating strategy ($CD3^{neg}/CD20^{neg}/CD19^{pos}/CD27^{hi}/CD38^{hi}/IgM^{neg}$) was applied to identify plasmablasts, and single plasmablasts were sorted into a 96-well PCR plate containing 10 µl of RNase-inhibiting catch buffer. Cloning of the variable domain of immunoglobulin derived from the single plasmablasts was performed as previously described[42,43]. Supernatants were collected from 293T cells co-transfected with the heavy chain and light chain variable domains inserted in plasmids designed to express human IgG1[43].

Expression of H7 and H3 haemagglutinins in MDCK-SIAT1 cells and production of single cycle virus pseudotypes for neutralization assays. MDCK-SIAT1 cells[34] were transduced to express a variety of H7 or H3 haemagglutinins with codon optimized sequences (Supplementary Table 5) and sorted by fluorescence-activated cell sorting (FACS) as described in ref. [31]. All high pathogenic H7 sequences had their polybasic cleavage sites removed and converted to the low pathogenic sequence of A/Anhui/1/2013 (PEIPKGRGLFGAI), which requires trypsin for cleavage in vitro. Pseudotypes were made by seeding haemagglutinin transduced cells with the signal sequence-inactivated single cycle influenza virus that has the H1 coding sequence of A/Puerto Rico/8/1934 replaced with an enhanced green fluorescent protein (eGFP) reporter[31,44]. In some cases the N1 sequence of A/Puerto Rico/8/1934 was replaced with the N2 of A/Victoria/361/2011 to optimize replication. Seed S-FLU viruses were doubly cloned and then expanded in the presence of trypsin on H7 haemagglutinin expressing MDCK-SIAT1 cells to provide single cycle viruses coated in the desired haemagglutinin (but that do not encode a viable haemagglutinin sequence) for use in neutralization assays in BSL-2 containment[45].

Initial screening of monoclonal antibodies. Antibodies were screened by either fluorescence microscopy or FACS staining. For fluorescence microscopy, various haemagglutinin-transduced MDCK-SIAT1 cells were distributed at 3×10^4 per well in 96-well flat-bottomed plates and incubated overnight. The medium was removed and supernatants from transfected 293T cells were added for 1 h, then cells were washed with PBS and developed with a goat anti-human IgG labelled with FITC (cat. no. H10301, Life Technologies) for 1 h. The wells were fixed with 1% formalin and binding antibodies detected by fluorescence microscopy.

For FACS staining, trypsinized MDCK-SIAT1 haemagglutinin-expressing cells were washed, resuspended in 96-well plates at 3×10^5 cells per well, and incubated with the antibody preparation for 1 h at 4 °C. Convalescent serum of H7N9-infected patients, day 28 serum of a 2013–2014 seasonal influenza vaccinee, and pandemic H1 head-specific antibody T3-11D[42] were used as controls. Cells without incubation with antibody and sera were included as controls. After washing, cells were incubated with goat anti-human IgG antibody conjugated with FITC (cat. no. 31628, Invitrogen) for 1 h at 4 °C. After washing, cells were examined using a FACSCalibur flow cytometer. For each sample at least 10,000 events were collected and analysed using FlowJo v.7 software (Tree Star).

The antibodies were tested for binding and neutralization of single cycle influenza coated in H3 and H7 haemagglutinins. Twelve representative neutralizing antibodies were expanded, purified and characterized in detail for their binding to H7 and H3, neutralizing and haemagglutination-inhibition activity against a variety of H7 and H3 pseudotypes and wild-type viruses.

Microneutralization of single cycle S-FLU pseudotyped with H7 proteins. Microneutralization assays based on the method of Rowe[46] were performed as described in detail previously[31,44]. Briefly, a saturating dose of the single cycle influenza virus S-FLU encoding an eGFP reporter[31,44] (50 µl), was mixed with titrated antibodies (50 µl) for 1 h, and then 3×10^4 indicator MDCK-SIAT1 cells were added (100 µl) and the mix was incubated at 37 °C overnight in 96-well plates. Neutralization was measured by suppression of eGFP or nucleoprotein expression in the indicator MDCK-SIAT1 cells, and EC_{50} (concentration of added antibody in 50 µl that suppressed eGFP expression by 50%) was calculated by linear interpolation. Cross-reactive anti-stem antibody MEDI8852[21] and anti-H3 head antibody Q11C9 (produced in house) were used as controls for microneutralization assays. In addition, post-infection mice sera were used as controls in the microneutralization assays for A/Netherlands/219/2003 and A/Guangdong/8H324/2017 pseudotypes.

Microneutralization of wild-type H7N9 viruses. In brief, MDCK cells cultured in 96-well plates were washed twice with PBS and incubated in 100 µl per well of medium without fetal bovine serum before the beginning of the experiment. The MAbs (starting at 0.8 mg ml^{-1}) were serially diluted twofold in triplicate, mixed with an equal volume of A/Guangdong/TH005/2017 (H7N9) or A/Anhui/1/2013 (H7N9) viruses, for which the virus titre was 100 $TCID_{50}$ (50% tissue culture infective dose). After incubation for 1 h at 37 °C, the mixture was added to MDCK cells for an additional 1 h incubation. The medium was then replaced with fresh medium supplemented with 2 µg ml^{-1} TPCK-trypsin with a subsequent incubation of 20 h at 37 °C. Both the virus control and cell control were included on each plate. The cell monolayers were then washed with PBS and fixed with cold acetone for 10 min. The viral antigen was detected by enzyme-linked immunosorbent assay using the mouse MAb against influenza A nucleoprotein (Medix Biochemica) and horseradish peroxidase conjugated goat anti-mouse IgG (Santa Cruz) as the primary antibody and secondary antibody, respectively. After being developed with tetramethylbenzydine (Sigma) chromogenic reagent, the optical density of each well was read at 490 nm (OD_{490}). Neutralizing activities of MAbs were expressed as EC_{50} determined by Graphpad Prism software version 5. A minimum of three independent repeats, an irrelevant antibody used as negative control, and a positive antibody used as positive control were included in the assay.

Haemagglutination-inhibition assay. Haemagglutination-inhibition assay was performed in V-bottomed plates, as described in the World Health Organization Manual on Animal Influenza Diagnosis and Surveillance WHO/CDS/CSR/NCS/2002.5 Rev.1[31]. Human red cells (1% vol/vol) were used for development, and the assay was read 1 h after the addition of red cells. The end point was recorded as the last dilution of antibody to give complete inhibition of agglutination, as defined by a clear tear drop pattern on tilting the plate. Tilted plates were photographed to confirm the end-points.

Selection of H7N9 escape mutants. Escape mutants of H7N9 A/Anhui/1/2013 were selected in a single-step protocol similar to that previously described[47]. Briefly, 50 µl of monoclonal antibody L4A-14 (1 mg ml^{-1}) was mixed with 50 µl of tenfold serially diluted LPAI H7N9 virus (stock virus of 1.72×10^6 p.f.u. ml^{-1}). The mixtures were incubated at 37 °C for 1 h before inoculation into 10-day-old embryonated chicken eggs at 35 °C for 48 h. The haemagglutinin-positive egg allantoic fluid with the lowest virus concentration was used to infect MDCK cells for single plaque picking. The plaque purified viruses were expanded once in MDCK cells. Viral RNA was extracted from the viruses using a QIAamp Viral RNA Mini kit (Qiagen) and reverse-transcribed to cDNA using a Verso cDNA synthesis kit (Thermo Scientific) with universal flu primer (sequence: 5′AGCAAAAGCAGG3′). The haemagglutinins were PCR-amplified using PfuUltra High-Fidelity DNA Polymerase (Agilent) by haemagglutinin-specific primers (5′AGCAAAAGCAGGGG3′ (forward); 5′AGTAGAAACAAGGGTGTTTT3′ (reverse)). The PCR products were then Sanger sequenced (Source Bioscience).

Haemagglutinin expression and purification. For the production of recombinant H7 haemagglutinin for crystallization, the codon-optimized ectodomain gene of haemagglutinin from A/Anhui/1/2013 was synthesized by Genewiz and cloned into the baculovirus transfer vector pFastBac1 (Invitrogen) in-frame with an N-terminal gp67 signal peptide for secretion, a C-terminal thrombin cleavage site, a trimeric foldon sequence to promote proper trimerization and a His6-tag at the extreme C terminus for purification. The recombinant baculovirus was prepared according to the Bac-to-Bac baculovirus expression system manual (Invitrogen)[48]. *Trichoplusia ni* (High Five) cells (Invitrogen) were infected with recombinant baculovirus at a multiplicity of infection of 0.5–10 at 27 °C for 48 h. The secreted soluble H7 haemagglutinin was recovered from cell supernatants by metal affinity chromatography using a HisTrap HP 5-ml column (GE Healthcare), then purified by ion-exchange chromatography using a Mono-Q 4.6/100 PE column (GE Healthcare). The purified proteins were subjected to thrombin treatment (Sigma, three units per mg haemagglutinin, overnight at 4 °C) to remove the C-terminal histidine tags. The proteins were further purified by subsequent size-exclusion gel filtration chromatography using a Superdex 200 16/60 GL column (GE Healthcare) with a running buffer (pH 8.0) of 20 mM Tris-HCl and 150 mM NaCl.

IgG expression and Fab preparation for crystallography. Full-length cDNA of the heavy chain and light chain of each H7-reactive antibody were codon-optimized, commercially synthesized (Genewiz) and inserted into the baculovirus transfer vector pFastBac-Dual (Invitrogen) for generation of IgG using the Bac-to-Bac baculovirus expression system. The heavy chain and light chain of each H7-reactive antibody were expressed under the control of p10 and polyhedrin promotors, respectively, given that the polyhedrin promotor is more powerful than the p10 promotor. Soluble IgG was harvested from the culture supernatants by Protein A affinity chromatography (GE Healthcare) and subsequently purified by gel filtration on a Hiload 16/60 Superdex200 PG column (GE Healthcare) in PBS buffer. The acquired IgG antibodies were used for functional evaluation during microneutralization, in the haemagglutination-inhibition assay and in the protection test in vivo.

To produce the Fab, antibodies were concentrated to ~20 mg ml^{-1} and digested using papain (cat. no. 20341, Pierece) protease at an antibody to papain ratio of 160:1 (wt/wt) at 37 °C for 6 h. The digestion mixture was loaded into a Protein A column (GE Healthcare) by applying the flow-through mode to separate the Fab fragment with the Fc region and undigested antibody. Fab fragments were collected, concentrated and purified to homogeneity by size-exclusion gel filtration chromatography (HiLoad 16/600 Superdex 200 pg, GE Healthcare) with PBS buffer.

Binding kinetics. The binding affinity of H7 haemagglutinin with antibody was measured by surface plasmon resonance using an BIAcore T100 device

(GE Healthcare) at room temperature (25 °C). The buffers for all proteins used for kinetic analysis were exchanged to PBST (consisting of PBS and 0.005% (vol/vol) Tween-20) via gel filtration. Goat anti-human antibody diluted at 20 μg ml^{-1} in 10 mM sodium acetate (pH 5.5) was immobilized on a CM5 sensor chip (CM-series sensor chips carrying a matrix of carboxymethylated dextran covalently attached to the gold surface, Biacore) with the standard 1-ethyl-3-(3-dimethylaminopropyl)-carbodiimide (EDC)/*N*-hydroxysuccinimide (NHS) coupling method to 7,000 response units (RU). Then, each of the human monoclonal anti-H7 antibodies diluted at 0.6 μg ml^{-1} in PBST was injected at a rate of 10 μl min^{-1} for 60 s, resulting in a final antibody-capturing density of 100 RU. Twofold dilutions (~15.6–500 nM for L4A-14 and L3A-44, and ~62.5–2,000 nM for L4B-18) of A/Anhui/1/2013 HA monomer were prepared and sequentially injected at a rate of 30 μl min^{-1} for 60 s, followed by a dissociation step for 120 s. After each cycle, a short injection of 10 mM NaOH was employed to regenerate the sensor surface. The association and disassociation curves were recorded, and the background binding was subtracted. The kinetic binding was analysed, and affinity constants were calculated using BIAcore T100 Evaluation software version 1.0.

Purification of the Fab-H7 complex. Fabs were mixed with purified A/Anhui/1/2013 haemagglutinin monomer protein at a molar stoichiometry of 1.5:1 to ensure saturation with Fab and then incubated on ice for 1 h. The complexes of Fab and HA protein were separated from unbound Fab by size-exclusion gel filtration chromatography and the buffer was changed to 20 mM Tris-HCl (pH 8.0) and 50 mM NaCl. The H7 haemagglutinin/Fab complexes were further concentrated to 10 mg ml^{-1} and used for subsequent crystallization studies.

Crystallization, data collection and structure determination. To define the epitopes on haemagglutinin of avian H7N9 virus, the crystal structures of L4A-14, L3A-44 and L4B-18, each in complex with H7 of A/Anhui/1/2013, were determined at resolutions of 3.3, 3.5 and 3.3 Å, respectively.

Crystallization trials were performed in sitting drops (1 μl + 1 μl) vapour diffusion at 4 and 18 °C. The crystallization conditions for the H7-antibody complex were as follows: L4A-14/H7, 0.2 M ammonium citrate tribasic pH 7.0, 20% wt/vol PEG3350, at 18 °C; L3A-44/H7, 0.2 M magnesium chloride hexahydrate, 0.1 M HEPES pH 7.5, 22% wt/vol poly(acrylic acid sodium salt) 5100, at 4 °C; L4B-18/H7, 35% vol/vol TacsimateTM pH 7.0, at 18 °C. Diffractable crystals were sent for X-ray analysis and the diffraction data were collected at Shanghai Synchrotron Radiation Facility (SSRF). For crystal diffraction, all crystals were cryo-protected by briefly soaking in reservoir solution supplemented with 20% (vol/vol) glycerol before flash-cooling in liquid nitrogen. All data sets were processed with HKL2000 software. The complex structures of H7 haemagglutinin and Fab were determined by the molecular replacement method with Phaser using the previously reported H7 protein structure of A/Anhui/1/2013 virus (PDB: 4KOL) and the Fab structure in the IL-17A/CAT-2200 Fab complex (PDB: 2VXS) as the search model. The atomic models were built with Coot and further rounds of refinement were completed with Phenix[49]. The stereochemical qualities of the final models were validated with MolProbity. Data collection and refinement statistics are summarized in Supplementary Table 6.

Animal study. Animal experiments were performed in accordance with the protocol approved by the Institutional Animal Care and Use Committee in the Genomics Research Center, Academia Sinica, Taiwan, the Institute of Microbiology, Chinese Academy of Sciences, China and the MRC Weatherall Institute of Molecular Medicine, University of Oxford, UK. The experiments were carried out in accordance with the 'Guide for the Care and Use of Laboratory Animals', the recommendations of the Institute for Laboratory Animal Research, and Association for Assessment and Accreditation of Laboratory Animal Care International standards.

The virus challenge with A/Guangdong/TH005/2017 (H7N9) was performed using six-week-old specific pathogen-free (SPF) female BALB/c mice (Vital River Laboratories). Mice were housed in biosafety level 3 bio-containment cages in the animal biosafety level 3 facilities. In the prophylactic studies, groups of five mice ($n = 5$) were passively inoculated with a dose of 10, 20 or 30 mg kg^{-1} of H7-reactive antibody (namely, L4A-14, L4B-18 and L3A-44) in a volume of 100 μl via intravenous injection 24 h before virus challenge. Mice in control groups were given an equal dose of anti-ebola MAb 13C6 as an antibody isotype control or an equivalent volume of PBS. For virus challenge, mice were anaesthetized and then intranasally inoculated with 100 median lethal dose (LD_{50}) of H7N9 A/Guangdong/TH005/2017 virus diluted with 50 μl PBS. In the therapeutic studies, groups of five mice were infected with 100 LD_{50} of A/Guangdong/TH005/2017 virus first, and then treated with a dose of 10, 20 or 30 mg kg^{-1} of H7-reactive antibody (L4A-14, L4B-18 and L3A-44) at 24 h post infection. Body weights and survival rates of mice were monitored and recorded for 14 days after infection. Survival rates were calculated based on institutional guidelines for defining dead mice as either actual death or displaying 25% or more loss of their initial body weight and subsequently euthanized. Animal care and housing were in compliance with ethical guidelines and approved by the Experimental Animal Ethic and Welfare Committee.

For challenge with A/Taiwan/1/2013, the A/Taiwan/1/2013 virus, a clinical strain collected from the first imported human H7N9 case in Taiwan in April 2013, was used. The H7N9 A/Taiwan/1/2013 virus is antigenically similar to the A/Anhui/1/2013 virus based on haemagglutination-inhibition assay data, which is consistent with the finding that their haemagglutinin sequences are closely related to each other[50]. Eight-week-old SPF BALB/c mice were purchased from BioLASCO Taiwan Co. and randomly distributed in experimental groups of six animals. These were anaesthetized with 0.2 ml intraperitoneal injection of 10× PBS-diluted Zoletil 50 (Virbac) injectable anaesthetic (tiletamine 2.5 mg ml^{-1}, zolazepam 2.5 mg ml^{-1}) prepared under aseptic conditions before virus infection. In the prophylaxis experiment, each group received a dose of intraperitonal antibodies (20 mg kg^{-1}) administration 24 h before intranasal infection with H7N9 A/Taiwan/1/2013 virus (5 LD_{50}). In the therapeutic experiment, each group received a dose of intraperitonal antibodies (20 mg kg^{-1}) 24 h after intranasal infection with A/Taiwan/01/2013 virus (5 LD_{50}). Mice in control groups were given an equal dose of anti-H1 head MAb T2-5D as an antibody isotype control or an equivalent volume of PBS. Baseline body weight and rectal temperature were recorded for each mouse on the day of infection. Body weight and rectal temperatures were recorded each day for 14 days after infection. Mice that fell below 70% of their initial (pre-infection) body weight were euthanized.

For the challenge with A/Aichi/2/1968-X31 H3N2 and A/California/7/2009-X179A H1N1 animals were purchased from Envigo RMS and housed in individually vented cages. Six- to eight-week-old DBA/2 (DBA/2OlaHsd) H2d and BALB/c (BALB/cOlaHsd) mice were used for X179A and X31 virus challenge experiments, respectively. After acclimatization, mice were given 10 mg kg^{-1} of antibody (intraperitoneally) in a 0.5 ml volume. After 24 h, mice were infected with either X179A or X31 virus (provided by the National Institute for Biological Standards and Control) at a dose of 10^4 $TCID_{50}$ and 32 haemagglutination unit (HAU), respectively. Virus infection was carried out on mice anaesthetized with isoflurane (Abbot) and 50 μl of virus given intranasally. Mice were weighed and scored throughout the study, and mice with 20% weight loss or morbid clinical scores were humanely killed.

Cell lines. 293T cells used for the production of S-FLU seed virus and human monoclonal antibodies were obtained from Sir William Dunn School of Pathology, University of Oxford and were not further authenticated. The ExpiCHO expression system used for the production of human MAbs in bulk was purchased from ThermoFisher and was not further authenticated. MDCK-SIAT1 cells were obtained from the European Collection of Cell Cultures distributed by Sigma (cat. no. 05071502) and were not further authenticated. *Trichoplusia ni* (High Five) cells were purchased from Invitrogen and were not further authenticated. All cell lines were tested for the presence of mycoplasma (MycoAlert Assay, Lonza and by Hoechst 33258 staining on A2H indicator cells (Sigma 85011441)) and were mycoplasma free.

Statistics. Graphs were presented using Microsoft Excel for Mac 2008 version 12.3.6, Microsoft PowerPoint for Mac 2008 for Mac version 12.3.6, BIAcore T100 Evaluation version 1.0 (GE Healthcare), HKL2000 and GraphPad Prism version 5 softwares. The statistical analyses were performed using GraphPad Prism version 5 and SPSS software version 20. A *P* value of less than 0.05 was considered significant.

Reporting Summary. Further information on research design is available in the Nature Research Reporting Summary linked to this article.

Data availability

The data that support the findings of this study are available from the corresponding authors upon request. Atomic coordinates for the H7-FabL4A-14, H7-FabL4B-18 and H7-FabL3A-44 complex as well as structure factors have been deposited to the Protein Data Bank under accession codes 6II4, 6II8 and 6II9.

Received: 22 May 2018; Accepted: 23 October 2018;
Published online: 26 November 2018

References

1. Wang, X. et al. Epidemiology of avian influenza A H7N9 virus in human beings across five epidemics in mainland China, 2013–17: an epidemiological study of laboratory-confirmed case series. *Lancet Infect. Dis.* **17**, 822–832 (2017).
2. Shi, J. et al. H7N9 virulent mutants detected in chickens in China pose an increased threat to humans. *Cell Res.* **27**, 1409–1421 (2017).
3. Yang, L. et al. Genesis and spread of newly emerged highly pathogenic H7N9 avian viruses in mainland China. *J. Virol.* **91**, e01277-17 (2017).
4. Zhang, F. et al. Human infections with recently-emerging highly pathogenic H7N9 avian influenza virus in China. *J. Infect.* **75**, 71–75 (2017).
5. Zhu, W. et al. Biological characterisation of the emerged highly pathogenic avian influenza (HPAI) A(H7N9) viruses in humans, in mainland China, 2016 to 2017. *Euro. Surveill.* **22**, 30533 (2017).
6. Qi, W. et al. Emergence and adaptation of a novel highly pathogenic H7N9 influenza virus in birds and humans from a 2013 human-infecting low-pathogenic ancestor. *J. Virol.* **92**, e00921-17 (2018).

7. Gao, R. et al. Human infection with a novel avian-origin influenza A (H7N9) virus. *N. Engl. J. Med.* **368**, 1888–1897 (2013).
8. Hu, Y. et al. Association between adverse clinical outcome in human disease caused by novel influenza A H7N9 virus and sustained viral shedding and emergence of antiviral resistance. *Lancet* **381**, 2273–2279 (2013).
9. Hai, R. et al. Influenza A(H7N9) virus gains neuraminidase inhibitor resistance without loss of in vivo virulence or transmissibility. *Nat. Commun.* **4**, 2854 (2013).
10. Lin, P. H. et al. Virological, serological, and antiviral studies in an imported human case of avian influenza A(H7N9) virus in Taiwan. *Clin. Infect. Dis.* **58**, 242–246 (2014).
11. Marjuki, H. et al. Neuraminidase mutations conferring resistance to oseltamivir in influenza A(H7N9) viruses. *J. Virol.* **89**, 5419–5426 (2015).
12. Imai, M. et al. A highly pathogenic avian H7N9 influenza virus isolated from a human is lethal in some ferrets infected via respiratory droplets. *Cell Host Microbe* **22**, 615–626 (2017).
13. Subbarao, K. Avian influenza H7N9 viruses: a rare second warning. *Cell Res.* **28**, 1–2 (2018).
14. *Summary of Influenza Risk Assessment Tool (IRAT) Results Web Site* (Centers for Disease Control and Prevention, accessed 2 May 2018); https://www.cdc.gov/flu/pandemic-resources/monitoring/irat-virus-summaries.htm.
15. Wang, D. et al. Two outbreak sources of influenza A (H7N9) viruses have been established in China. *J. Virol.* **90**, 5561–5573 (2016).
16. Kile, J. C. et al. Update: increase in human infections with novel Asian lineage avian influenza A(H7N9) viruses during the fifth epidemic—China, October 1, 2016–August 7, 2017. *MMWR. Morb. Mortal. Wkly Rep.* **66**, 928–932 (2017).
17. Gostic, K. M., Ambrose, M., Worobey, M. & Lloyd-Smith, J. O. Potent protection against H5N1 and H7N9 influenza via childhood hemagglutinin imprinting. *Science* **354**, 722–726 (2016).
18. Ekiert, D. C. et al. A highly conserved neutralizing epitope on group 2 influenza A viruses. *Science* **333**, 843–850 (2011).
19. Guo, L. et al. Human antibody responses to avian influenza A(H7N9) virus, 2013. *Emerg. Infect. Dis.* **20**, 192–200 (2014).
20. Dunand, C. J. et al. Preexisting human antibodies neutralize recently emerged H7N9 influenza strains. *J. Clin. Invest.* **125**, 1255–1268 (2015).
21. Kallewaard, N. L. et al. Structure and function analysis of an antibody recognizing all influenza A subtypes. *Cell* **166**, 596–608 (2016).
22. Yamayoshi, S. et al. Human protective monoclonal antibodies against the HA stem of group 2 HAs derived from an H3N2 virus-infected human. *J. Infect.* **76**, 177–185 (2018).
23. Stadlbauer, D. et al. Vaccination with a recombinant H7 hemagglutinin-based influenza virus vaccine induces broadly reactive antibodies in humans. *mSphere* **2**, e00502-17 (2017).
24. Stadlbauer, D., Nachbagauer, R., Meade, P. & Krammer, F. Universal influenza virus vaccines: what can we learn from the human immune response following exposure to H7 subtype viruses? *Front. Med.* **11**, 471–479 (2017).
25. Andrews, S. F. et al. Preferential induction of cross-group influenza A hemagglutinin stem-specific memory B cells after H7N9 immunization in humans. *Sci. Immunol.* **2**, eaan2676 (2017).
26. Wang, Z. et al. Recovery from severe H7N9 disease is associated with diverse response mechanisms dominated by $CD8^+$ T cells. *Nat. Commun.* **6**, 6833 (2015).
27. Baz, M. et al. Nonreplicating influenza A virus vaccines confer broad protection against lethal challenge. *mBio* **6**, e01487-15 (2015).
28. Sutton, T. C. et al. Protective efficacy of influenza group 2 hemagglutinin stem-fragment immunogen vaccines. *NPJ Vaccines* **2**, 35 (2017).
29. Sobhanie, M. et al. Evaluation of the safety and immunogenicity of a candidate pandemic live attenuated influenza vaccine (pLAIV) against influenza A(H7N9). *J. Infect. Dis.* **213**, 922–929 (2016).
30. Dunand, C. J. et al. Both neutralizing and non-neutralizing human H7N9 influenza vaccine-induced monoclonal antibodies confer protection. *Cell Host Microbe* **19**, 800–813 (2016).
31. Powell, T. J., Silk, J. D., Sharps, J., Fodor, E. & Townsend, A. R. Pseudotyped influenza A virus as a vaccine for the induction of heterotypic immunity. *J. Virol.* **86**, 13397–13406 (2012).
32. Burke, D. F. & Smith, D. J. A recommended numbering scheme for influenza A HA subtypes. *PLoS ONE* **9**, e112302 (2014).
33. Thornburg, N. J. et al. H7N9 influenza virus neutralizing antibodies that possess few somatic mutations. *J. Clin. Invest.* **126**, 1482–1494 (2016).
34. Matrosovich, M., Matrosovichm, T., Carr, J., Roberts, N. A. & Klenk, H. D. Overexpression of the alpha-2,6-sialyltransferase in MDCK cells increases influenza virus sensitivity to neuraminidase inhibitors. *J. Virol.* **77**, 8418–8425 (2003).
35. Wiley, D. C. & Skehel, J. J. The structure and function of the hemagglutinin membrane glycoprotein of influenza virus. *Annu. Rev. Biochem.* **56**, 365–394 (1987).
36. Chen, C. et al. Structural insight into a human neutralizing antibody against influenza virus H7N9. *J. Virol.* **92**, e01850-17 (2018).
37. Shi, Y. et al. Structures and receptor binding of hemagglutinins from human-infecting H7N9 influenza viruses. *Science* **342**, 243–247 (2013).
38. Ohshima, N. et al. Naturally occurring antibodies in humans can neutralize a variety of influenza virus strains, including H3, H1, H2, and H5. *J. Virol.* **85**, 11048–11057 (2011).
39. Lee, P. S. et al. Receptor mimicry by antibody F045-092 facilitates universal binding to the H3 subtype of influenza virus. *Nat. Commun.* **5**, 3614 (2014).
40. McCarthy, K. R. et al. Memory B cells that cross-react with Group 1 and Group 2 influenza A viruses are abundant in adult human repertoires. *Immunity* **48**, 174–184 (2018).
41. Ekiert, D. C. et al. Cross-neutralization of influenza A viruses mediated by a single antibody loop. *Nature* **489**, 526–532 (2012).
42. Huang, K. Y. et al. Focused antibody response to influenza linked to antigenic drift. *J. Clin. Invest.* **125**, 2631–2645 (2015).
43. Smith, K. et al. Rapid generation of fully human monoclonal antibodies specific to a vaccinating antigen. *Nat. Protoc.* **4**, 372–384 (2009).
44. Xiao, J. H. et al. Characterization of influenza virus pseudotyped with Ebolavirus glycoprotein. *J. Virol.* **92**, e00941-17 (2018).
4. Martínez-Sobrido, L. et al. Hemagglutinin-pseudotyped green fluorescent protein-expressing influenza viruses for the detection of influenza virus neutralizing antibodies. *J. Virol.* **84**, 2157–2163 (2010).
46. Rowe, T. et al. Detection of antibody to avian influenza A (H5N1) virus in human serum by using a combination of serologic assays. *J. Clin. Microbiol.* **37**, 937–943 (1999).
47. Peacock, T. et al. Antigenic mapping of an H9N2 avian influenza virus reveals two discrete antigenic sites and a novel mechanism of immune escape. *Sci. Rep.* **6**, 18745 (2016).
48. Zhang, W. et al. Crystal structure of the swine-origin A (H1N1)-2009 influenza A virus hemagglutinin (HA) reveals similar antigenicity to that of the 1918 pandemic virus. *Protein Cell* **1**, 459–467 (2010).
49. Aad, G. et al. Search for new particles in two-jet final states in 7Â TeV proton-proton collisions with the ATLAS detector at the LHC. *Phys. Rev. Lett.* **105**, 161801 (2010).
50. Yang, J.-R. et al. Characterization of influenza A (H7N9) viruses isolated from human cases imported into Taiwan. *PLoS ONE* **10**, e0119792 (2015).

Acknowledgements

The authors acknowledge support from the laboratories that provided the sequences of reference antibody MEDI8852[21] for the comparisons in the tables and figures. The authors also acknowledge the BD FACSAria cell sorter service provided by the Core Instrument Center of Chang Gung University, and C. Waugh for FACS sorting B cells and MDCK-SIAT1 cell lines at WIMM Oxford. These studies were funded by the Townsend-Jeantet Charitable Trust (registered charity no. 1011770), the Emergency Technology Research Issue on Prevention and Control for Human infection with A (H7N9) Avian Influenza Virus (10600100000015001206), the Strategic Priority Research Program of the Chinese Academy of Sciences (CAS) (XDB29010000), the National Science and Technology Major Project (2018ZX10101004), the Human Immunology Unit (MRC), Oxford University, Chang Gung Medical Research Program (CMRPG3G0921, CMRPG3G0922) and the Ministry of Science and Technology of Taiwan (MOST 104-2320-B-182A-002-MY2, MOST 105-2320-B-182A-008- and MOST 107-2321-B-182A-003-). G.F.G. is supported partly as a leading principal investigator of the NSFC Innovative Research Group (81621091). Y.S. is supported by the Excellent Young Scientist Program from the National Natural Science Foundation of China (81622031), the Excellent Young Scientist Program of CAS and the Youth Innovation Promotion Association CAS (2015078).

Author contributions

K.-Y.A.H., G.F.G., Y.S. and A.R.T. conceived and designed the study. K.-Y.A.H., P.R., H.J., B.W., L.S., T.D., Y.-M.L., P.C., M.I., M.-C.W., Z.C., R.S., C.-C.H., J.-H.Y., J.Q., T.-Y.L., A.L., T.J.P., J.-T.J., C.M., G.F.G., Y.S. and A.R.T. carried out the experiments. K.-Y.A.H., P.R., H.J., B.W., L.S., T.D., Y.-M.L., J.-T.J., C.M., G.F.G., Y.S. and A.R.T. performed data analysis and figure/table preparation. K.-Y.A.H., P.R., G.F.G., Y.S. and A.R.T. wrote the manuscript.

Competing interests

The authors declare no competing interests.

Additional information

Supplementary information is available for this paper at https://doi.org/10.1038/s41564-018-0303-7.

Reprints and permissions information is available at www.nature.com/reprints.

Correspondence and requests for materials should be addressed to K.-Y.A.H. or G.F.G. or Y.S. or A.R.T.

Publisher's note: Springer Nature remains neutral with regard to jurisdictional claims in published maps and institutional affiliations.